ELSEVIER

Journal of Quantitative Spectroscopy & Radiative Transfer 99 (2006) 341–348

Journal of Quantitative Spectroscopy & Radiative Transfer

www.elsevier.com/locate/jqsrt

K-shell radiation physics in low- to moderate-atomic-number z-pinch plasmas on the Z accelerator

B. Jones[a,*], C. Deeney[a], C.A. Coverdale[a], P.D. LePell[b], J.L. McKenney[a], J.P. Apruzese[c], J.W. Thornhill[c], K.G. Whitney[c], R.W. Clark[c], A.L. Velikovich[c], J. Davis[c], Y. Maron[d], V. Kantsyrev[e], A. Safronova[e], V.I. Oreshkin[f]

[a]*Sandia National Laboratories, Albuquerque, NM 87185, USA*[1]
[b]*Ktech Corporation, Albuquerque, NM 87123, USA*
[c]*Naval Research Laboratory, Washington, DC 20375, USA*
[d]*Faculty of Physics, Weizmann Institute of Science, 76100 Rehovot, Israel*
[e]*Department of Physics, University of Nevada, Reno, NV 89557-0058, USA*
[f]*High Current Electronics Institute, Tomsk, Siberia 634055, Russia*

Accepted 26 April 2005

Abstract

Dense z-pinches produced by 100 ns implosions of wire arrays or gas puffs produce substantial soft X-ray power. One class of z-pinch radiation sources includes low- to moderate-atomic-number K-shell radiators, such as aluminum and iron. These loads are designed for 1–10 keV K-shell X-ray generation, and offer opportunities for crystal spectroscopy that can reveal fundamental properties of the plasma when studied using plasma spectroscopic modeling. Typically these plasmas are characterized by ion densities of $\sim 10^{20}$ cm^{-3}, diameters of 1–5 mm, electron temperatures up to several keV, and a range of opacities of the K-shell lines. Measurements from wire arrays on Sandia's 20 MA Z accelerator are presented along with

*Corresponding author. Tel.: +1 505 284 9481; fax: +1 505 845 7685.
E-mail address: bmjones@sandia.gov (B. Jones).

[1]Sandia is a multi-program laboratory operated by Sandia Corporation, a Lockheed Martin Company, for the United States Department of Energy's National Nuclear Security Administration under Contract DE-AC04-94AL85000.

0022-4073/$ - see front matter
doi:10.1016/j.jqsrt.2005.05.027

collisional radiative and hydrodynamic simulations. The impact of opacity and 3D structure on non-LTE, non-diffusive radiation transport and X-ray production is discussed.

Keywords: Z-pinch plasma; K-shell X-ray production and spectroscopy; Opacity

1. Introduction

Pulsed-power-driven fast z-pinches are efficient generators of soft X-rays, with ~15% conversion of input electrical energy to radiation. In recent years, Sandia's Z accelerator [1] has produced X-ray powers >250 TW by driving 20 MA in 100 ns through an annular array of several hundred fine tungsten wires [2]. Strong $\mathbf{j} \times \mathbf{B}$ forces implode the wire array, which generates nearly 2 MJ of X-rays in <10 ns when it stagnates as a high-energy-density plasma column on the array axis. These 150–200 eV blackbody-like radiators [3] are presently used for inertial confinement fusion studies and other work.

Another class of z-pinch radiation sources includes wire arrays and gas puffs designed to generate K-shell X-ray emission from low- to moderate-atomic-number elements (ranging from Al to Cu on Z). These plasmas offer radiation physics regimes distinct from high-atomic-number tungsten wire arrays, and provide 1–10 keV K-shell X-ray emission for spectroscopy, radiation transport investigations, and atomic physics analysis using non-LTE population kinetics codes. With ion densities $n_i \sim 10^{20}\,\mathrm{cm}^{-3}$ and electron temperatures up to several keV, opacity often plays a significant role in K-shell radiation transport over the millimeter path lengths, though not enough to justify radiation diffusion models.

Besides radiation transport, the fundamental ionization and excitation are not simple to treat. For electron collisional rates to greatly exceed radiative rates for complete LTE [4], a hydrogen-like plasma's electron density must be $n_e > 3.9 \times 10^{17}\,\mathrm{cm}^{-3} Z^6 (T_e/13.6\,\mathrm{eV})^{1/2} \approx 7 \times 10^{24}\,\mathrm{cm}^{-3}$ for Al with charge state $Z = 12$ and electron temperature $T_e = 500$ eV. Thus, this class of z-pinch typically neither has atomic level populations in LTE, nor can it be treated with a coronal equilibrium model [5] which would require $n_e < 5.9 \times 10^{10}\,\mathrm{cm}^{-3} Z^6 T_e^{1/2} \exp(0.1Z^2/T_e) \approx 4 \times 10^{18}\,\mathrm{cm}^{-3}$ in the case of Al K-shell for collisional deexcitation of ions to be dominated by radiative decay. For these plasma more detailed population kinetics models are required [6].

In this paper, we review experimental results from wire array z-pinch K-shell sources fielded on the Z accelerator, and compare them with collisional radiative equations (CRE) and hydrodynamic simulations which treat the complex radiation processes inherent to these plasmas. Physical processes impacting X-ray production, including opacity and three-dimensional (3D) dynamics, will be discussed in the context of optimizing K-shell radiation performance.

2. Design of z-pinch loads for K-shell radiation

K-shell production is driven by considerations that lead to wire array design distinct from those used in the generation of soft X-rays from tungsten loads. It is necessary to achieve significantly higher electron temperatures (i.e. ~500 eV for Al, ~3 keV for stainless steel) in the stagnated pinch

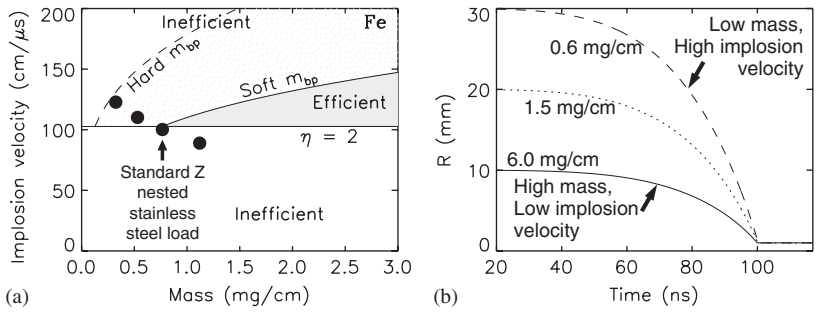

Fig. 1. (a) K-shell scaling theory in wire array mass/length and implosion velocity space for iron. 55-mm diameter nested stainless steel loads on Z (circles) nearly access an efficient K-shell radiation regime, which is the region bracketed by the soft m_{bp} and the $\eta = 2$ line. (b) Moderate-atomic-number wire array K-shell sources must have larger diameter and lower mass to implode with enough velocity to exceed the $\eta = 2$ cutoff. Calculated radial trajectories of wire arrays are shown as a function of time, assuming cylindrically symmetric implosion of an infinitely thin shell.

in order to ionize the wire material to the K shell, which places constraints on the load geometry and the photon energy accessible on a fast driver of a given peak current I.

Scaling laws for the K-shell yield have been developed using one-dimensional (1D) radiation-magneto-hydrodynamic (RMHD) simulations [7–9]. These atomic-number-dependent models guide the design of K-shell sources on Z, as illustrated in Fig. 1(a) for Fe, by predicting a region of efficient K-shell generation in wire array initial mass/length and final implosion velocity space. The ratio of the kinetic energy per imploding ion to the energy needed to ionize to the K shell (η) must be at least greater than 2 in order to generate a suitable pinch temperature to strip the ions to the K shell collisionally. In addition, the strong density dependence of K-shell excitation requires that a mass threshold be met, shown as the soft mass break-point (m_{bp}) for 1D RMHD modeling with a phenomenological turbulence model included or as the hard m_{bp} without it [8]. Below the mass threshold, K-shell yield scales as m^2(or equivalently I^4) while in an efficient regime it scales linearly with mass (or as I^2) [10].

These cutoffs move toward higher mass and velocity with increasing atomic number, and Fig. 1(a) indicates that the Z accelerator is not quite able to access efficient K-shell radiation for iron (stainless steel wire arrays produce 50 kJ, 10 TW). A pulsed-power generator of given current is capable of delivering a certain kinetic energy to an imploding z-pinch, and thus can only produce efficient K-shell emission in elements up to a particular atomic number (including Al and Ti for the Z machine in this model). Exceeding the $\eta = 2$ cutoff generally requires increasing the wire array diameter and decreasing the mass in order to increase the implosion velocity, as in thin-shell implosion trajectory calculations in Fig. 1(b); a standard W array on Z has 6 mg/cm on 20 mm diameter, while stainless steel is typically 1 mg/cm on 55-mm diameter.

3. Opacity and the role of gradients in dense non-LTE z-pinches

The temperatures and densities produced in these z-pinch plasmas result in large optical depths in the low-atomic-number K-shell lines. This is clearly seen in time-resolved spectra for a nested

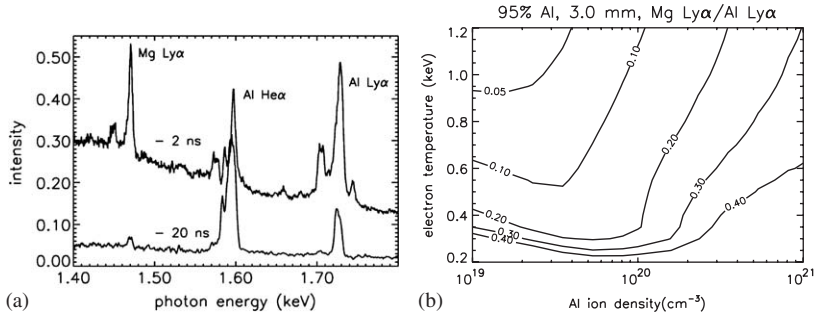

Fig. 2. (a) Time-resolved spectra from Z811 (95% Al, 5% Mg) showing opacity clamping of Al Ly−α line to similar intensity as Mg Ly−α. (b) CRE-modeled Mg/Al Ly−α line ratio contours quantify the impact of opacity versus T_e and n_i.

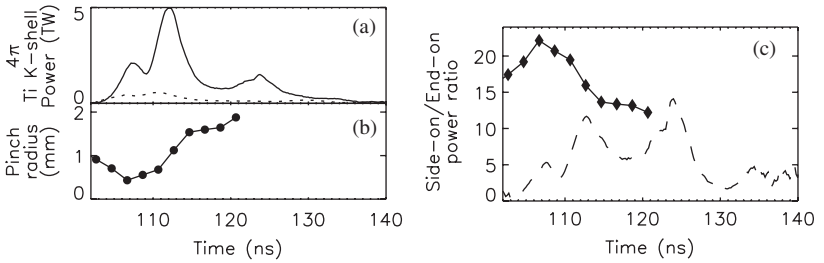

Fig. 3. Ti K-shell power from Z888 (Ni/Ti on Al mixed nested array) shows pinch transition from volume to surface radiator due to opacity. (a) Power radiated into 4π inferred from side-on (solid) versus end-on (dotted) measurements. These are equal for an optically thin volume radiator. (b) Pinch radius measured with X-ray pinhole camera. (c) Side-on/end-on power ratio (dashed) from data in (a) and also $2\pi rL/\pi r^2$ (diamonds) using $r(t)$ from (b) which is the power ratio for a surface radiator.

Al 5056 wire array (95% Al, 5% Mg; 40 and 20 mm array diameters, with 1.0 and 0.5 mg/cm). If the plasma were optically thin, one would expect to see a Mg/Al Ly−α line ratio of 5%, but Fig. 2(a) shows that at 2 ns before peak X-ray power, the observed ratio is 40%. This is due to the large optical depth of the Al Ly−α line, and can be quantified with non-LTE CRE modeling [6,11,12]. Fig. 2(b) shows contours of the Mg to Al Ly−α ratio for a 3-mm-diameter uniform plasma, which approach 5% for low n_i and high T_e but are significantly greater particularly for higher densities. Quantitative determination of n_i is obtained from measured K-shell power and pinch diameter coupled to CRE modeling, with T_e then determined from K-shell line ratio measurements and n_i [11]. This time-resolved modeling accounts for opacity by ray-traced radiation transport over photon energy bins that adequately resolve the K-shell lines, and reproduces the effect of opacity on the observed spectrum consistent with experimental data.

Another clear indication of opacity is the difference in K-shell power inferred in side-on (viewing perpendicular to the z-pinch axis) versus end-on (viewing along the z-axis) measurements obtained with filtered diamond photoconducting detectors [13] on a Ni/Ti on Al nested wire array. The inferred Ti K-shell power emitted into 4π solid angle is shown in Fig. 3(a), while Fig. 3(b) shows the corresponding evolution of the z-pinch radius $r(t)$ from an end-on X-ray

pinhole camera. The ratio of side-on to end-on power from (a) is shown in Fig. 3(c). An optically thin volume radiator would radiate the same power in any viewing angle, and in fact this ratio is ~1 early in time. This ratio quickly becomes >1, however, as increased optical thickness in the end-on viewing direction (greater length of integration) prohibits photons from escaping along the z-axis resulting in lower end-on power. For a completely optically thick surface radiator, this ratio would be $2\pi rL/\pi r^2$, which is plotted in Fig. 3(c) using $r(t)$ from (b). The curves in (c) best agree at peak K-shell power, when the pinch is assembled on axis and n_i is greatest. They are never equal, however, indicating that while opacity plays a significant role in the K-shell radiation transport, the plasma is not completely opaque and thus transport calculations more detailed than radiation diffusion are required.

A third indication of opacity in dense z-pinches is the observation of absorption lines in the emitted K-shell spectrum. Fig. 4(a) shows a space- and time-integrated spectrum from a 6 mg/cm, 20-mm diameter Al 5056 wire array. The absorption features seen adjacent to the Mg and Al He−α lines indicate the presence of spatial gradients in temperature or density. To address these features, CRE modeling of Al was performed in the manner of [14,15] assuming a $T_e = 1$ keV, $n_i = 6.5 \times 10^{20}$ cm^{-3} plasma core of radius 2.5 mm, surrounded by a 45 eV, 3.2×10^{20} cm^{-3}, 62-μm thick blanket. These core parameters represent a best-fit obtained by comparing the modeled H-like lines and continuum above the H-edge to the experiment, while the blanket parameters were chosen phenomenologically to reproduce He-like emission and some absorption features. Fig. 4(b) shows the modeled optical thicknesses (τ) in these two layers. Innershell absorption due to satellite lines is capable of providing $\tau > 2$, leading to reabsorption in the cold blanket surrounding the hot core as seen in the experiment. Similar analysis indicates cold plasma surrounding a hot core in Sandia's 8 MA Saturn accelerator; CRE and radiation transport modeling was matched to measured Al spectra to determine best-fit $n_i(r)$ and $T_e(r)$, both peaked on axis [16].

This analysis provides an example of how opacity can compromise the K-shell yield in a z-pinch [17]. This experiment produced 110 kJ Al K-shell, while 400 kJ is typical of a 1.5 mg/cm Al wire array on Z. This reduction is likely due to reduced implosion velocity, but also to reabsorption of the K-shell photons in a cold, outer blanket. Fig. 5(a) shows the temperature and density profiles of this blanket at the time of peak K-shell emission as calculated by a 1D RMHD simulation benchmarked to reproduce the 110 kJ K-shell experimental yield. Post processing this profile with a detailed multifrequency radiation transport model [18] that includes innershell absorption

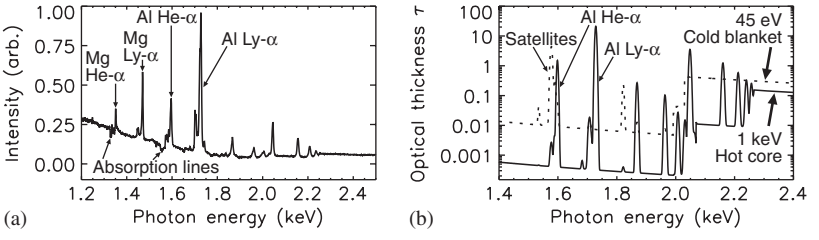

Fig. 4. (a) Z427 time-integrated spectrum showing absorption features adjacent to Mg and Al He−α lines. (b) Modeled Al optical thicknesses in cold blanket (dashed) and hot core (solid); innershell absorption occurs in blanket due to He−α satellites.

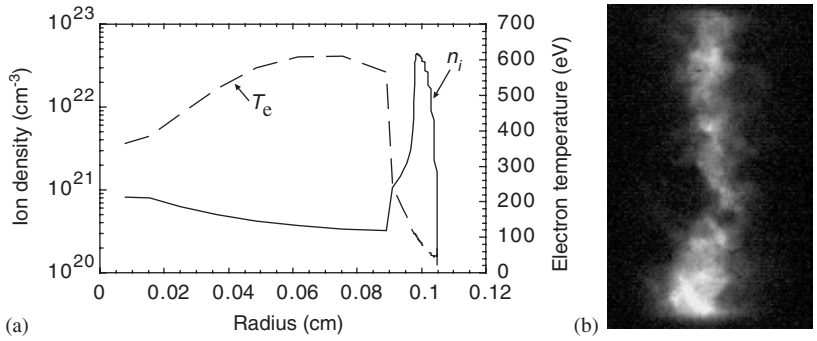

Fig. 5. (a) 1D RMHD model of Z427 Al z-pinch, showing evolution of a cold, dense, absorbing blanket surrounding the hot core. (b) Z427 K-shell X-ray pinhole camera image showing 3D structure; absorbing regions of plasma surround a radiating core.

opacity, which was neglected in the original calculation, gives negligible K-shell emission. Innershell absorption is especially important for high mass pinches of low-atomic-number elements such as Al [17]. The fact that reduced but significant K-shell emission was observed may be a product of 3D structure formed by MHD turbulence in the z-pinch, that is, breaks in the opaque blanket could allow K-shell photons to escape the core. This is supported by the K-shell X-ray pinhole image in Fig. 5(b), which appears to show regions of absorbing plasma partially masking a 1.0-mm-radius brightly emitting core at 2 ns before peak K-shell power.

4. Conclusions, discussion, and future directions

Low- to moderate-atomic-number, hot, dense z-pinches can be efficient radiators of K-shell photons, and they provide rich opportunities for radiation transport, non-LTE population kinetics and plasma physics studies. The potential for high opacity in the K-shell lines and their non-LTE nature require detailed CRE and radiation transport modeling to provide understanding of X-ray production and z-pinch dynamics. The peak current of a pulsed-power driver generally limits the maximum atomic number that can efficiently radiate in the K shell. The Z machine can nearly access the calculated efficient regime for iron, which should be attained when Z is modified to the 27 MA Z-Refurbishment accelerator in 2006.

High opacity in efficiently radiating, i.e., Al, plasmas can limit the K-shell yield, and must be considered in scaling these sources to higher-current generators requiring higher-mass loads [17]. This effect is reduced for higher atomic numbers [19]; however, radiative transfer must still be treated carefully to calculate the emission spectrum and infer plasma parameters accurately [6].

Nested wire arrays of mixed materials have been proposed to mitigate reabsorption by surrounding the radiating z-pinch core with a blanket of a different material, transparent to the K-shell photons generated on axis [17,20]. The 4 MA Double-EAGLE facility demonstrated a K-shell yield increase in Mg-coated Al wires by this mechanism [21]. Mixed nested Al and Ti arrays have been fielded on Z [22,23] to improve Ti K-shell yields, and also to study interaction of the arrays through dopant spectroscopy [24]. Axially localized low-atomic-number coated dopants

may allow K-shell spectroscopic determination of n_i and T_e in a tungsten z-pinch, and measurement of particle transport due to MHD turbulence in initial tests on the 1 MA Zebra accelerator. Spectroscopic modeling of coated materials supports this continuing effort.

Additional problems presently being studied include non-equilibrium higher-atomic-number z-pinches for which CRE techniques might not be applicable, and the impact of L-shell radiative energy loss [25,26] on the implosion dynamics prior to stagnation. Doppler shifts due to velocity gradients could complicate radiation transport, and may affect ongoing efforts to extract ion temperatures from measured line widths [27]. High ion temperatures are expected in these plasmas due to the large initial kinetic energy input during stagnation, and may affect plasma heating and opacity.

The physics of radiation transport may at some level be intertwined with the plasma physics of 3D structure arising from MHD implosion instabilities. While the magneto-Rayleigh–Taylor instability may limit the total X-ray power produced by causing a distributed arrival of material on the axis during stagnation [28], it is interesting to consider that this structure may benefit K-shell transport by breaking up an opaque blanket surrounding the hot core. Seeded perturbations in wire array z-pinches could potentially augment this effect by intentionally opening holes in the blanket [29]. Ongoing diagnostic development efforts on Z, including elliptical crystal spectrometry [30] and monochromatic self-emission imaging [31], seek to address the complicated interplay between radiation transport and 3D structure that can arise.

As z-pinch simulations coupling 3D MHD, CRE and detailed radiation transport remain computationally prohibitive, a continuing challenge is to identify problems that are both tractable and illuminate physical phenomena of importance. K-shell emission from low- to moderate-atomic-number pinches provides an opportunity for studying non-LTE population kinetics (with complex dependencies on atomic, collision as well as plasma physics) and radiation transport in a regime dominated by these issues.

References

[1] Spielman RB, Deeney C, Chandler GA, Douglas MR, Fehl DL, Matzen MK, et al. Phys Plasmas 1998;5:2105–11.
[2] Deeney C, Douglas MR, Spielman RB, Nash TJ, Peterson DL, L'Eplattenier P, et al. Phys Rev Lett 1998;81:4883–6.
[3] Cuneo ME, Vesey RA, Porter JL, Chandler GA, Fehl DL, Gilliland TL, et al. Phys Plasmas 2001;8:2257–67.
[4] Griem HR. Principles of Plasma Spectroscopy. Cambridge: Cambridge University Press; 1997. p. 214.
[5] DeMichelis C, Mattioli M. Nucl Fusion 1981;21:677–754.
[6] Davis J, Clark R, Blaha M, Giuliani JL. Laser Part Beams 2001;19:557–77.
[7] Whitney KG, Thornhill JW, Apruzese JP, Davis J. J Appl Phys 1990;67:1725–35.
[8] Thornhill JW, Whitney KG, Deeney C, LePell PD. Phys Plasmas 1994;1:321–30.
[9] Whitney KG, Thornhill JW, Giuliani JL, Davis J, Miles LA, Nolting EE, et al. Phys Rev E 1994;50:2166–74.
[10] Thornhill JW, Whitney KG, Davis J. JQSRT 1990;44:251–9.
[11] Apruzese JP, Whitney KG, Davis J, Kepple PC. JQSRT 1997;57:41–61.
[12] Apruzese JP, Davis J, Whitney KG, Thornhill JW, Kepple PC, Clark RW, et al. Phys Plasmas 2002;9:2411–9.
[13] Spielman RB. Rev Sci Instrum 1992;63:5056–8.
[14] Gregorian L, Bernshtam VA, Kroupp E, Davara G, Maron Y. Phys Rev E 2003;67:016404-1-6.
[15] Ralchenko YV, Maron Y. JQSRT 2001;71:609–21.
[16] Apruzese JP, Thornhill JW, Whitney KG, Davis J, Deeney C, Coverdale CA. Phys Plasmas 2001;8:3799–809.

[17] Thornhill JW, Whitney KG, Davis J, Apruzese JP. J Appl Phys 1996;80:710–8.
[18] Clark RW, Davis J, Apruzese JP, Giuliani JL. JQSRT 1995;53:307–20.
[19] Apruzese JP. In: Drobot AT, editor. Computer applications in plasma science and engineering. New York: Springer; 1991. p. 359–80.
[20] Apruzese JP, Davis J. J Appl Phys 1985;57:4349–53.
[21] Deeney C, LePell PD, Failor BH, Wong SL, Apruzese JP, Whitney KG, et al. Phys Rev E 1995;51:4823–32.
[22] Jones B, Deeney C, Coverdale CA, LePell PD, Apruzese JP, Whitney KG, et al. In: 14th IEEE pulsed power conference. Dallas: IEEE; 2003. p. 115.
[23] LePell PD, Coverdale CA, Deeney C, Maron Y. Bull Am Phys Soc 2003;48:237.
[24] Deeney C, Apruzese JP, Coverdale CA, Whitney KG, Thornhill JW, Davis J. Phys. Rev. Lett. 2004;93:155001/1-4.
[25] Davis J, Giuliani JL, Mulbrandon M. Phys Plasmas 1995;2:1766–74.
[26] LePell PD, Hansen SB, Shlyaptseva AS, Coverdale C, Deeney C, Apruzese JP, et al. Phys Plasmas 2005;12:032701/1–13.
[27] LePell PD, Deeney C, Coverdale C, Jones B, Meyer C, Apruzese J. Bull Am Phys Soc 2004;49:200.
[28] Chittenden JP, Lebedev SV, Jennings CA, Bland SN, Ciardi A. Plasma Phys Control Fusion 2004;46:B457–76.
[29] Jones B, Deeney C, McKenney JL, Garasi CJ, Mehlhorn TA, Robinson AC, et al. Submitted to Phys Rev Lett 2005.
[30] Lake PW, Bailey JE, Rochau GA, Moore TC, Petmecky D, Gard P. Rev Sci Instrum 2004;75:3690–2.
[31] Jones B, Deeney C, Pirela A, Meyer C, Petmecky D, Gard P, et al. Rev Sci Instrum 2004;75:4029–32.